Physics-Informed Neural Networks for Multiphysics Simulations: Application to Coupled Electromagnetic-Thermal Modeling

Shutong Qi [1], Costas D. Sarris [2]
The Edward S. Rogers Sr. Department of Electrical and Computer Engineering
University of Toronto, Toronto, ON, Canada
[1]st.qi@mail.utoronto.ca, [2]costas.sarris@utoronto.ca

***Abstract*— We demonstrate a new approach to building multiphysics solvers, employing physics-informed neural networks (PINNs), through the example of coupled electromagnetic-thermal simulations. In this example, the well-known Finite-Difference Time-Domain (FDTD) method for electromagnetic field simulation is combined with a PINN, designed to replace a thermal solver. The PINN is trained in an unsupervised manner by implementing the heat equation and boundary conditions into the network. As a result, the cost of generating "ground truth" data is eliminated. Our work enables standalone electromagnetic simulators, like FDTD, to solve multiphysics problems accurately and efficiently.**

***Keywords*— Multiphysics simulation, FDTD, neural networks, unsupervised learning.**

I. Introduction

Multiphysics interactions of electromagnetic fields have been at the forefront of research in the microwave community [1], [2], [3] and beyond [4]. The numerical study of these interactions is based on coupling electromagnetic field simulators with independently developed solvers of associated thermal, mechanical, quantum and chemical phenomena. Fundamental questions of numerical accuracy, stability and efficiency, thoroughly yet separately addressed over the years for computational methods in electromagnetics, acoustics, thermodynamics, mechanics, quantum mechanics and chemistry, have received little attention in the process of integrating them into multiphysics packages. However, there are multiple mechanisms for error propagation between coupled multiphysics numerical techniques [5] and challenges with respect to producing optimal meshes for coupled discrete methods [6].

This paper proposes an alternative route to formulating multiphysics solvers, inspired by recent advances in scientific machine learning and the emergence of physics-informed neural networks (PINNs) [7]. PINNs are neural network architectures aimed at solving partial differential equations and inverse problems, with a wide range of successful applications. We employ PINNs to solve the heat equation based on initial conditions generated by the Finite-Difference Time-Domain (FDTD) method for Maxwell's equations, for coupled electromagnetic-thermal problems. Our approach combines a robust, error-controlled numerical technique, such as FDTD, with a PINN as a heat equation solver. Thus, we bypass the need to use, configure and generate a new mesh for a thermal solver, or to re-use the FDTD mesh for the solution of the heat equation (a sub-optimal approach that is commonly used in the literature [8]).

The rest of the paper explains how to use this approach to extract the steady-state temperature distribution in lossy, inhomogeneous media, excited by microwave fields (Fig. 1). We train a physics-informed U-Net (PIUN) in an unsupervised manner, i.e. with no need for "ground truth" data generation. Numerical results demonstrate the accuracy and efficiency of this combination that effectively turns FDTD into a multiphysics simulator. Similar steps can be used to couple any electromagnetic simulator to governing equations for other types of multiphysics interactions of electromagnetic fields.

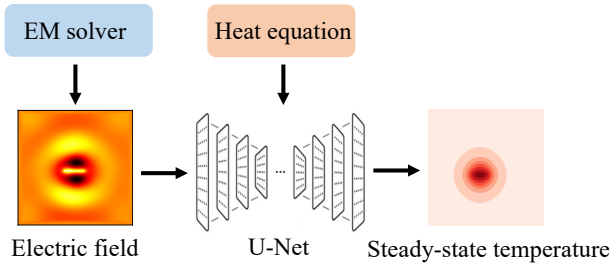

Fig. 1. The flowchart of the proposed method.

II. Problem Statement

Fig. 2 shows the general class of two-dimensional problems we consider, where a lossy, arbitrarily shaped region is embedded in a host dielectric medium. We consider the case of transverse magnetic polarized fields, with (H_x, H_y, E_z) field components, determined by an FDTD simulation, applying standard finite-difference update equations such as:

$$E_{i,j}^{z,n+1} = \frac{\frac{\varepsilon_{i,j}}{\Delta t} - \frac{\sigma_{i,j}}{2}}{\frac{\varepsilon_{i,j}}{\Delta t} + \frac{\sigma_{i,j}}{2}} E_{i,j}^{z,n} + \frac{1}{\frac{\varepsilon_{i,j}}{\Delta t} + \frac{\sigma_{i,j}}{2}} \cdot \left(\frac{H_{i+\frac{1}{2},j}^{y,n+\frac{1}{2}} - H_{i-\frac{1}{2},j}^{y,n+\frac{1}{2}}}{\Delta x} - \frac{H_{i,j+\frac{1}{2}}^{x,n+\frac{1}{2}} - H_{i,j-\frac{1}{2}}^{x,n+\frac{1}{2}}}{\Delta y} \right), \tag{1}$$

$$H_{i,j+\frac{1}{2}}^{x,n+\frac{1}{2}} = H_{i,j+\frac{1}{2}}^{x,n-\frac{1}{2}} + \frac{\Delta t}{\mu} \frac{E_{i,j+1}^{z,n} - E_{i,j}^{z,n}}{\Delta y}, \tag{2}$$

$$H_{i+\frac{1}{2},j}^{y,n+\frac{1}{2}} = H_{i+\frac{1}{2},j}^{y,n-\frac{1}{2}} - \frac{\Delta t}{\mu} \frac{E_{i+1,j}^{z,n} - E_{i,j}^{z,n}}{\Delta x}, \tag{3}$$

where (i, j) are Yee cell indices, n is the time step index, $\varepsilon_{i,j}$ and $\sigma_{i,j}$ are the permittivity and conductivity of the (i, j) cell of dimensions $\Delta x \times \Delta y$, respectively, and μ is the uniform magnetic permeability throughout the domain of Fig. 2. The presence of an electromagnetic field in the conducting medium results in dissipated (ohmic) volume power density Q, which can be determined from FDTD at each (i, j) Yee cell as:

$$Q_{i,j} = \sigma_{i,j} \langle |\mathbf{E}_{i,j}|^2 \rangle \tag{4}$$

where $\langle \cdot \rangle$ denotes time average. In turn, Q is a heat source whose effect on the temperature within the medium can be found by solving the heat equation, which is written, in the presence of a cooling fluid circulating inside the medium, as follows:

$$\rho C_p \frac{\partial T}{\partial t} = Q + \nabla \cdot (k \nabla T) + V_s (T_b - T) \tag{5}$$

where ρ is the material density, C_p is the heat capacity, T is the temperature, Q is the power density of the heat source and k is the heat conductivity. Moreover, V_s is the product of flow and heat capacity of the cooling fluid and T_b is the temperature of the cooling fluid. These parameters are assumed to be time-independent in this paper, although our work can be readily extended to the time-dependent case. Instead of setting up a finite-difference solver for (5), we extract the solution through a physics-informed U-Net, as shown next.

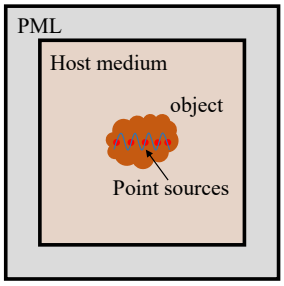

Fig. 2. Computational domain for the geometries considered in this paper.

III. A PIUN for the Heat Equation

A U-Net is an encoder-decoder structure that is efficient in solving image-to-image problems [9]. It consists of a down-sampling route and an up-sampling route, with several convolutional blocks in each route. The detailed U-Net structure can be found in [10]. In this work, the down-sampling route extracts the object geometries and domain properties from the input data and transforms them into a higher dimensional representation through the convolutional blocks. The up-sampling route reconstructs these extracted features and exports the steady-state temperature distribution based on the embedded heat equation and the boundary conditions. We implement the steady-state version of (5):

$$Q + k\nabla^2 T + V_s (T_b - T) = 0, \tag{6}$$

along with its associated boundary conditions into the PIUN. In particular, we use (6) to formulate a loss function for the PIUN:

$$L_{PIUN} = \left| Q + k\nabla^2 T + V_s (T_b - T) \right|^2. \tag{7}$$

Then, the PIUN optimizes its parameters through backpropagation to minimize (7) for a given dissipated power density (Q) and heat conductivity (k), in an unsupervised manner, as shown in Fig. 3.

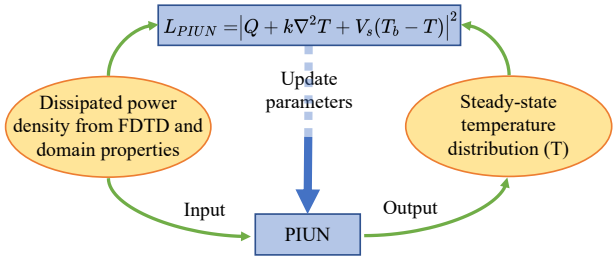

Fig. 3. Implementation of the heat equation as loss function.

We can also readily implement boundary conditions into the PIUN. For example, consider the Robin boundary condition:

$$-k \left(\frac{\partial T}{\partial \mathbf{n}} \right)_w = h \left(T_w - T_f \right) \tag{8}$$

where $\partial T / \partial \mathbf{n}$ is the partial derivative of T in the normal direction defined by $\mathbf{n}$, w represents the position of the boundary, h is the convective heat transfer coefficient, T_w is the boundary temperature and T_f is the external temperature. In the x-direction, (8) can be discretized as:

$$-k \left(\frac{T_{i,j} - T_{i-1,j}}{\Delta x} \right) = h \left(\frac{T_{i,j} + T_{i-1,j}}{2} - T_f \right), \tag{9}$$

where $T_{i,j}$ represents the temperature at the boundary and $T_{i-1,j}$ is the temperature on the left of $T_{i,j}$. Then, the temperature at an (i, j) node is

$$T_{i,j} = \frac{(2k - h\Delta x) T_{i-1,j} + 2h\Delta x T_f}{2k + h\Delta x}. \tag{10}$$

The boundary temperature (10) can be directly embedded into the neural network architecture along with the U-Net. Then, we can compute the temperature of the entire computational domain by combining the output from the U-Net with the boundary temperature from (10).

The proposed PIUN can be trained in an unsupervised way based on the heat equation and boundary conditions. Except for the higher efficiency compared to the supervised training, the proposed unsupervised approach has improved generalizability, since the PIUN learns from the embedded heat equation, instead of the training data. Then, any problem based on (6) can be solved by the PIUN. Note that the electromagnetic source amplitude and material properties only affect the dissipated power density (Q) in this problem. Hence, the proposed approach is generalizable with respect to geometry, source excitation and material properties.

IV. Numerical Results

In this section, the proposed PIUN is verified through two-dimensional simulations for the steady-state temperature distribution in a lossy object within a host medium excited by an electromagnetic wave (Fig. 2). In the training cases of the PIUN, the lossy objects are circullar, elliptical or consisting of overlapping circles and ellipses. We introduce multiple objects in the computational domain for testing purposes. When generating the objects, the radius of circles, the major/minor axes of ellipses, and the center of each object are all variables used to diversify the geometry training set of the PIUN.

In Fig. 2, the FDTD computational domain is a square with a side length 138.66 mm, partitioned into 148×148 Yee cells. The surrounding 10 cells belong to a perfectly matched layer (PML) [11]. An array of point sources is used as a source excitation. The region of the thermal simulation is the same as the FDTD computational domain, excluding the PML. Instead, the Robin boundary condition (10) is applied to the output temperature from the PIUN, with a heat transfer coefficient $h = 5\,\mathrm{W/m^2/K}$ [12].

In our experiments, the operation frequency is 2 GHz. At this frequency, the relative permittivity, ε_r, of the object is in the range of $[20.1, 23.2]$ and $[62.0, 65.1]$, the relative permeability $\mu_r = 1$, and the electric conductivity, σ, is in the range of $[0.83, 1.10]$ and $[4.1, 4.2]$ (S/m). For the host medium, ε_r is in the range of $[8.1, 8.2]$, $\mu_r = 1$, and σ is in the range of $[0.43, 0.57]$ (S/m). The heat conductivity of the host medium is $0.5\,(\mathrm{W/m/K})$, and $[0.56, 0.60]\,(\mathrm{W/m/K})$ for the object.

We build a dataset containing 1000 sets of training data and 200 sets of testing data. Training data include single homogeneous and inhomogeneous objects, while testing data have multiple objects in the computational region. So, the testing geometries are generalized versions of the training ones, with enhanced complexity. Some representative geometries from the training and testing sets are shown in Fig. 4, where different colors represent different material properties.

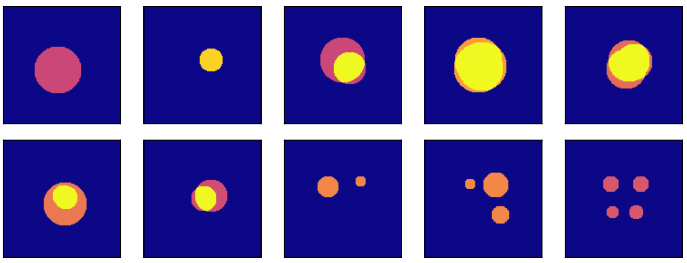

Fig. 4. Samples of training (first line) and testing (second line) geometries.

The inputs of the PIUN are the dissipated power density $Q\,(\mathrm{W/m^3})$, computed by FDTD, and the heat conductivity $k\,(\mathrm{W/m/K})$ of the computational domain. For each input case, the output of the PIUN is the steady-state temperature distribution in the computational domain. To evaluate the accuracy of the prediction, we use a forward-time centered-space (FTCS) based thermal solver [13] to generate ground-truth data for the testing cases. To clarify, these ground-truth data are generated for validation purposes, *not for training*, since the training is unsupervised. The relative error ($\mathcal{E}_{rel}$) is computed by:

$$\mathcal{E}_{rel} = \frac{1}{N_x N_y} \sum_{i=1}^{Nx} \sum_{j=1}^{Ny} \frac{|T_p(i,j) - T_r(i,j)|}{T_r(i,j) - T_b}, \qquad (11)$$

where T_p is the prediction from the PIUN, T_r is the result from FTCS, T_b is the external temperature, N_x and N_y represent the number of cells in the x and y direction. The mean relative error of the whole testing set is 3.68×10^{-4} for the trained PIUN. Fig. 5 shows several testing cases for the PIUN.

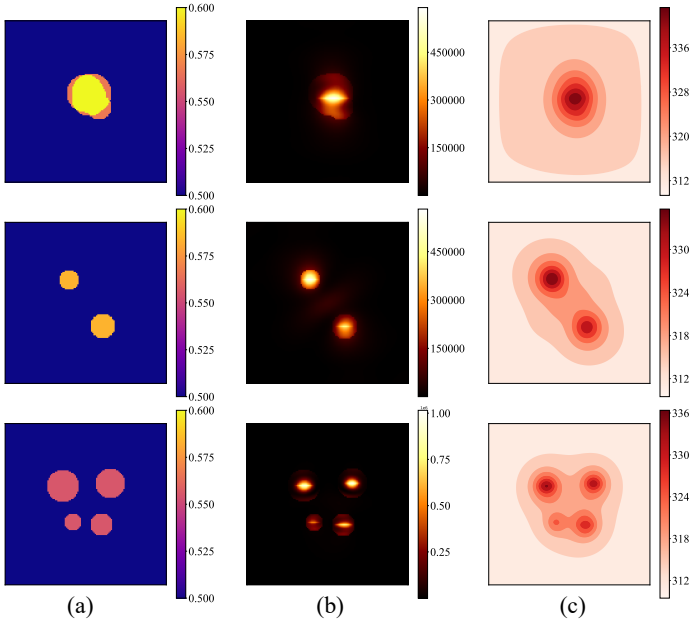

Fig. 5. Testing cases for the PIUN, showing: (a) heat conductivity $k\,(\mathrm{W/m/K})$, (b) dissipated power density $Q\,(\mathrm{W/m^3})$, and (c) predicted temperature distribution $T\,(\mathrm{K})$.

It takes on average 0.031 seconds for the PIUN to produce one steady-state temperature distribution on an Intel-i5 CPU. On the other hand, the FTCS method takes 22.74 seconds to simulate one testing case on the same CPU. Besides, COMSOL Multiphysics (a finite element method solver) takes 9.13 seconds to simulate such two-dimensional cases with the default mesh (23394 cells in total). These comparisons show the excellent computational efficiency of the proposed PIUN.

V. Conclusion

We demonstrated the feasibility of coupling FDTD to a neural network for electromagnetic-thermal analysis. The proposed network, a PIUN, replaced a thermal solver to produce the steady-state temperature distribution in geometries involving arbitrarily shaped lossy dielectrics within host media, accurately and efficiently. Thus, electromagnetic-thermal problems were solved by a single FDTD solver combined with the PIUN. Moreover, the PIUN was trained in an unsupervised

manner, eliminating the cost of generating ground-truth data. This work is a promising step towards PINN-based multiphysics solvers for a wide range of applications, including electrothermal analysis of integrated circuits and design optimization of hyperthermia applicators.

REFERENCES

[1] F. Apollonio, M. Liberti, A. Amadei, M. Aschi, M. Pellegrino, M. D'Alessandro, M. D'Abramo, A. Di Nola, and G. d'Inzeo, "Mixed quantum-classical methods for molecular simulations of biochemical reactions with microwave fields: The case study of myoglobin," *IEEE Trans. Microwave Theory Tech.*, vol. 56, no. 11, pp. 2511–2519, 2008.

[2] W. Strohbehn and E. Douple, "Hyperthermia and cancer therapy: A review of biomedical engineering contributions and challenges," *IEEE Trans. on Biomed. Engineering*, vol. 31, no. 12, p. 779–787, Dec. 1984.

[3] W. Zhang, F. Feng, V.-M.-R. Gongal-Reddy, J. Zhang, S. Yan, J. Ma, and Q.-J. Zhang, "Space mapping approach to electromagnetic centric multiphysics parametric modeling of microwave components," *IEEE Trans. Microwave Theory Tech.*, vol. 66, no. 7, pp. 3169–3185, 2018.

[4] M. A. Miri, F. Ruesink, E. Verhagen, and A. Alù, "Optical non-reciprocity based on optomechanical coupling," *Phys. Rev. Applied*, vol. 7, no. 6, p. 064014, June 2017.

[5] K. Wilczynski, M. Olszewska-Placha, and M. Celuch, "Application of conformal mapping to rigorous validation of 2D coupled EM-CFD modelling," in *2020 IEEE MTT-S Int. Microwave Symp. Dig.*, 2020, pp. 154–157.

[6] F. L. Teixeira, "Compatible discretizations for multiphysics: A brief review and some future challenges," in *Proc. IEEE AP-S Int. Symp. on Antennas and Propagat.*, 2016, pp. 1289–1290.

[7] G. E. Karniadakis, I. G. Kevrekidis, L. Lu, P. Perdikaris, S. Wang, and L. Yang, "Physics-informed machine learning," *Nat. Rev. Phys.*, vol. 3, no. 6, pp. 422–440, 2021.

[8] F. Torres and B. Jecko, "Complete FDTD analysis of microwave heating processes in frequency-dependent and temperature-dependent media," *IEEE Trans. Microwave Theory Tech.*, vol. 45, no. 1, pp. 108–117, 1997.

[9] O. Ronneberger, P. Fischer, and T. Brox, "U-net: Convolutional networks for biomedical image segmentation," in *Int. Conf. Medical Image Comp. and Computer-Assisted Interv.* Springer, 2015, pp. 234–241.

[10] S. Qi, Y. Wang, Y. Li, X. Wu, Q. Ren, and Y. Ren, "Two-dimensional electromagnetic solver based on deep learning technique," *IEEE J. on Multiscale and Multiphysics Comp. Tech.*, vol. 5, pp. 83–88, 2020.

[11] J.-P. Berenger, "A perfectly matched layer for the absorption of electromagnetic waves," *J. Comput. Phys.*, vol. 114, no. 2, pp. 185–200, 1994.

[12] A. Chanmugam, R. Hatwar, and C. Herman, "Thermal analysis of cancerous breast model," in *ASME International Mechanical Engineering Congress and Exposition*, vol. 45189. ASME, 2012, pp. 135–143.

[13] W. Thiel, K. Tornquist, R. Reano, and L. P. B. Katehi, "A study of thermal effects in RF-MEM-switches using a time domain approach," in *2002 IEEE MTT-S Int. Microwave Symp. Dig.*, vol. 1, 2002, pp. 235–238.